

# Optical phase modulation using a hybrid carbon nanotube-liquid-crystal nanophotonic device

Ranjith Rajasekharan-Unnithan, Haider Butt, and Timothy D. Wilkinson\*

Department of Engineering, Centre of Molecular Materials for Photonics and Electronics, University of Cambridge, 9 J.J. Thomson Avenue, Cambridge CB3 0FA, UK

\*Corresponding author: tdw13@cam.ac.uk

Received January 26, 2009; revised February 27, 2009; accepted March 4, 2009;  
posted March 13, 2009 (Doc. ID 106822); published April 10, 2009

The carbon nanotube-liquid-crystal (CNT-LC) nanophotonic device is a class of device based on the hybrid combination of a sparse array of multiwall carbon nanotube electrodes grown on a silicon surface in a liquid-crystal cell. The multiwall carbon nanotubes act as individual electrode sites that spawn an electric-field profile, dictating the refractive index profile within the liquid crystal and hence creating a series of graded index profiles, which form various optical elements such as a simple microlens array. We present the refractive index and therefore phase modulation capabilities of a CNT-LC nanophotonic device with experimental results as well as computer modeling and potential applications. © 2009 Optical Society of America

OCIS codes: 230.0230, 230.3720, 350.4238, 350.4600.

The electro-optic properties of a liquid crystal can be modified by introducing nanoparticles [1,2]. Carbon based nanoparticles are found to be promising because of the excellent electrical properties and strong interaction with the aromatic mesogenic groups of liquid crystals. Jeong *et al.* [3] showed the formation of unusual double-four-lobe nematic textures in a carbon nanotube-doped liquid crystal under the application of an external voltage. From the hybrid combination of carbon nanotubes and liquid crystals, it has been found that there is a strong interaction between carbon nanotubes and liquid crystals despite the size difference between liquid-crystal molecules (1–2 nm) and carbon nanotubes (a few nanometers to micrometers). This interaction can be interpreted as an optical interaction through the optical anisotropy of the liquid crystal. Hence carbon nanotubes attached to a surface of a substrate in the liquid-crystal cell can be used to form electrodes and defect centers in the medium, and the liquid crystal can be manipulated by applying an external electric field. Based on this technique, an electrically reconfigurable nanophotonic device has been fabricated with light modulation capability [4]. The carbon nanotube electrode arrays were grown on silicon substrates by plasma-enhanced chemical vapor deposition after employing e-beam lithography to nickel catalyst layer into an array. This allowed the growth of a single multiwall carbon nanotube of around 50 nm diameter at each point in the array [4]. In some devices, the nanotubes were patterned in small groups of four with a 1  $\mu\text{m}$  spacing between the nanotubes and 10  $\mu\text{m}$  spacing between the groups. The nanotubes array was then assembled with a top electrode containing indium tin oxide on 0.5-mm-thick borosilicate glass into a liquid-crystal cell with a 20  $\mu\text{m}$  cell gap set by spacer balls in UV glue. In this Letter we discuss the optical phase modulation using these devices with the experimental data and computer simulation while discussing the potential applications.

The refractive index profile across the device was varied by changing the orientation of the liquid-

crystal molecules with different applied voltages. When carbon nanotube electrodes were immersed in a planar-aligned nematic liquid-crystal material [(a positive dielectric anisotropy nematic liquid-crystal mixture BL048 from Merck, which has a low refractive index  $n_o$  ( $n_o=1.5277$ ) for light polarized perpendicular to its optic axis and a high refractive index  $n_e$  ( $n_e=1.7904$ ) for light polarized along the optic axis] with no electric field applied, then the liquid-crystal molecules aligned parallel to the upper substrate surfaces owing to the planar alignment given by rubbing a surface coating (a thin film of polyimide) with a defect surrounding the nanotube as shown in Fig. 1(a). When a potential difference was applied between individual nanotubes and a ground plane, an electric field was generated, and the field profile from the tube tip to the ground plane appears approximately Gaussian in shape [5]. The electric field interacts with the dielectric anisotropy of the liquid-crystal molecules and forces them to align in the direction of electric field. The liquid-crystal molecules are finally oriented in a quite complex geometry owing to the Gaussian field profile combined with the surface effects of the alignment layer (AM4276) applied to the upper substrate of the cell. The result of these two effects creates a varying or gradient refractive index profile across the device. The refractive index profile formed is in effect a micro-optical element due to the gradient index profile across the reoriented liquid crystal under the electric field. The phase modulation

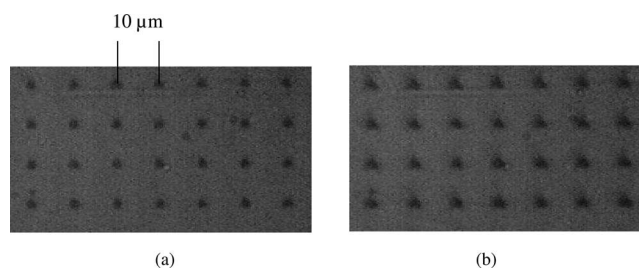


Fig. 1. Device switching at two different voltages: (a)  $V=0$  Vrms, (b)  $V=6$  Vrms.

capabilities of the micro-optical elements can be tuned by varying the applied field and thereby reorienting the liquid-crystal molecules to create a new graded refractive index profile and varying the optical properties of the micro-optical element.

The fabricated device was viewed under a reflective optical microscope using a polarizer and analyzer. The arrays of nanotube electrodes are clearly visible as black dots on the device because of the defects created by the nanotubes in the nematic liquid crystal. The device at two different voltages is shown in Fig. 1. The sparse array at zero voltage is shown in Fig. 1(a). The arrays of carbon nanotube (CNT) groups were clearly visible as defects in the image. When the applied field was increased, the arrays of nanotube electrodes were seen to begin switching at 0.6 Vrms, equivalent of a Fredrickzs transition. It was observed that above 1 Vrms the nanotube arrays were all fully switched, as shown in Fig. 1(b). The aperture size of each lenslet was found to increase with respect to the applied voltage up to a limiting size of 10  $\mu\text{m}$ , and further increase in voltage distorted the refractive index profile of lenslets.

Three-dimensional phase recovery from the nanophotonics device is essential for studying the phase modulation capabilities of the device. The phase was retrieved from the device using interference techniques [6]. A Fourier-transform-based fringe analysis [7–9] was used to retrieve the phase from the device, as it requires only one interferogram and gives higher accuracy by eliminating the background intensity distribution, speckle noise, and optical noise from higher spatial frequencies. The nanophotonic device was characterized using a modified Fourier transform technique. By using the above technique,

the microscopic phase profile of each lenslet was recovered using an interference setup constructed with an optical microscope.

The microscopic phase profile of each lenslet is of interest as it decides the real modulation capability and applications of the device. The experimental setup consisted of a He–Ne laser along with a beam expander as the illuminating source. An optical microscope was used to detect the beam in reflective mode and for capturing the image. An eye piece having a magnification of  $\times 20$  was used in the microscope. The device was mounted on a fine three-axis tilting stage and attached to the microscope. The rubbing direction of the device was kept at  $45^\circ$  to the polarizer. The interference fringes were formed owing to the interference between the ordinary and extraordinary beams being combined by an analyzer that was crossed with polarizer [10]. A rotating diffuser (transparent plastic sheet) was used to average out speckle noise. The fringes were captured by a CCD camera and frame grabber. The interferogram, retrieved unwrapped phase profile of an array of lenslet, and one lenslet at different voltages are shown in Fig. 2. It was found that in the absence of an external voltage circular fringes were observed, which showed an alignment deformation of the liquid-crystal molecules near the carbon nanotubes, even though the macroscopic alignment was planar [Fig. 2(a)]. The change in phase modulation (the phase difference between the center and circumference of lenslet) was bigger at lower voltages than at higher voltages, as shown in Fig. 2(a), because the molecular alignment was more or less homeotropic at higher voltages, resulting in the diminishing of the interference fringes [Fig. 2(a)]. The phase profile was distorted at 0 Vrms

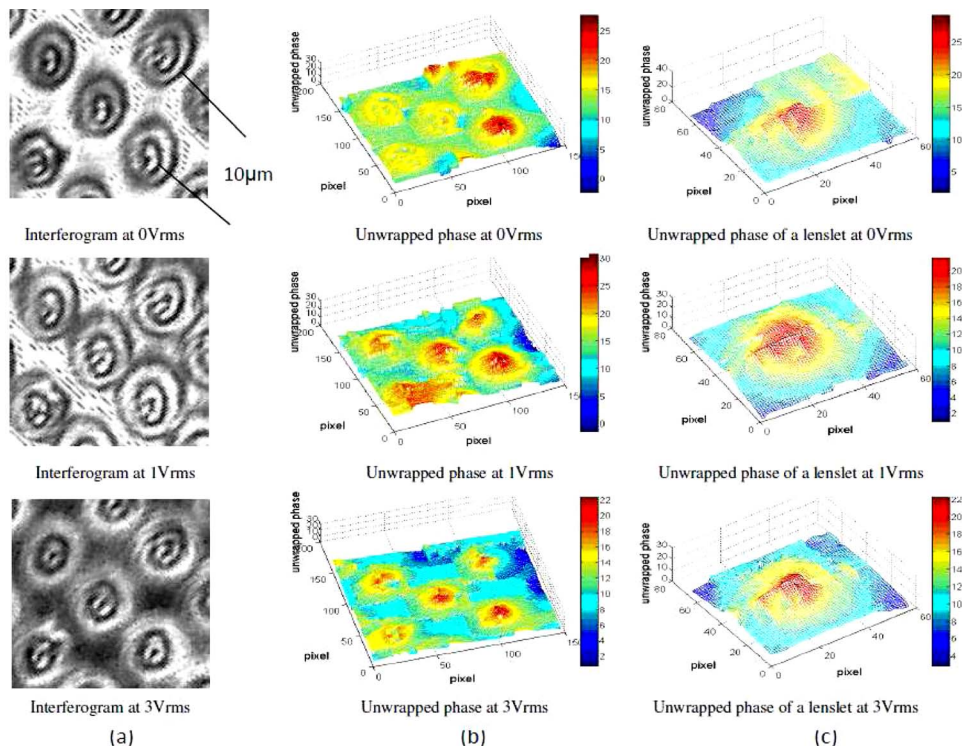


Fig. 2. (Color online) 3D microscopic phase profile of an array at 0 Vrms, 1 Vrms, and 3 Vrms: (a) an array of interferograms, (b) unwrapped phase of the array, (c) unwrapped phase of a lenslet.

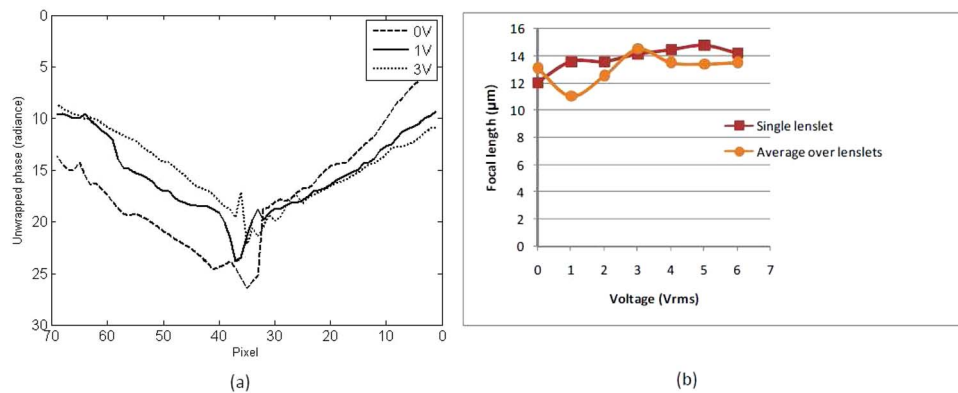


Fig. 3. (Color online) (a) 2D unwrapped phase profile at 0 Vrms, 1 Vrms, and 3 Vrms. (b) Focal length variation with respect to external voltage.

but became symmetric at 1 Vrms, and distortion again started from 3 Vrms upwards for the device [11], as shown in Fig. 3(a). The focal length was calculated using the equation  $f = \rho^2 / 2OPD$  [12,13], where OPD is the peak-to-valley optical path difference from the center to the edge and  $\rho$  is the radius of the test area ( $5 \mu\text{m}$ ). The variation in the focal length of a single lenslet and average over lenslets in a particular area of the device with respect to voltage is shown in Fig. 3(b). The focal length of each lenslet at 0 Vrms is randomly varied. It was observed that the focal length increased with respect to the voltage, and hence the lenslets were concave in nature. The focal length variation was in agreement with the simulation results, where the Gaussian profile gave maximum alignment at the center of each lenslet compared with the circumference. An average focal length over the lenslets were calculated, because the focal length variation was found to be random after 3 Vrms for many lenslets, and also there was a slight change in the focal length between each lenslet below 3 Vrms in some areas of the device. This is because of the complicated electric field profile due to different ohmic contact for each CNT.

The CNT-liquid-crystal nanophotonic device can be used as an electrically reconfigurable optical diffuser. Optical diffusers change the angular divergence of incident light as well as act as a random phase modulator. At the same time the current device acts as a grating because of the periodically arranged CNTs at  $10 \mu\text{m}$  separation and microlenses due to the liquid crystal. Thus the device can be used for homogenous illumination that is reconfigurable with an external voltage. The device has over  $1000 \times 1000$  lenslets within the  $10 \text{ mm} \times 10 \text{ mm}$  area. From geometric optics, the greater the number of element in the lens array, the finer the separation of the incident beam and hence the more uniform illumination [13]. The lenslets in the device are not completely similar in performance, which helps to suppress the multiple beam interference patterns due to the spots generated by each lenslet. This can further enhance the uniformity of illumination [14].

The phase modulation capabilities of the device were tuned by varying the applied field and thereby reorienting the liquid-crystal molecules and hence

varied the optical properties of the microlens array. The fabricated device has a resolution of over  $1000 \times 1000$  lenslets and a size of  $10 \text{ mm} \times 10 \text{ mm}$ . The device performance was elaborated while explaining the potential applications.

The authors thank Philip Hands, Christoph Bay, and Jon Freeman for the fruitful discussions. Ranjith. R specially thanks UK-India Education and Research Initiative (UKIERI, British Council) and Cambridge Commonwealth Trust (CCT) for giving funding to pursue PhD.

## References

1. W. Lee, C.-Y. Wang, and Y.-C. Shih, *Appl. Phys. Lett.* **85**, 513 (2004).
2. O. Trushkevych, N. Collings, T. Hasan, V. Scardaci, A. C. Ferrari, T. D. Wilkinson, W. A. Crossland, W. I. Milne, J. Geng, B. F. G. Johnson, and S. Macaulay, *J. Phys. D* **41**, 125106 (2008).
3. S. J. Jeong, P. Sureshkumar, K.-U. Jeong, A. K. Srivastava, S. H. Lee, S. H. Jeong, Y. H. Lee, R. Lu, and S.-T. Wu, *Opt. Express* **15**, 11698 (2007).
4. T. D. Wilkinson, Xiaozhi Wang, Ken B. K. Teo, and William I. Milne, *Adv. Mater. (Weinheim, Ger.)* **20**, 363 (2008).
5. W. I. Milne, K. B. K. Teo, M. Chhowalla, G. A. J. Amaratunga, S. B. Lee, D. G. Hasko, H. Ahmed, O. Groening, P. Legagneux, L. Gangloff, J. P. Schnell, G. Pirio, D. Pribat, M. Castignolles, A. Loiseau, V. Semet, and V. Thien Binh, *Diamond Relat. Mater.* **12**, 422 (2003).
6. P. Hariharan, *Optical Interferometry* (Academic, 1985), pp. 157–159.
7. C. Roddier and F. Roddier, *Appl. Opt.* **26**, 1668 (1987).
8. J. William and W. Macy, *Appl. Opt.* **22**, 3898 (1983).
9. M. Takeda, H. Ina, and S. Kobayashi, *J. Opt. Soc. Am.* **72**, 156 (1982).
10. M. Ye, Y. Yokoyama, and S. Sato, *Appl. Phys. Lett.* **89**, 141112 (2006).
11. H. Ren and S. T. Wu, *Opt. Express* **15**, 11328 (2007).
12. H. Ren, Y. H. Fan, and S. T. Wu, *Appl. Phys. Lett.* **82**, 22 (2003).
13. G. Li, D. Mathine, P. Valley, P. Åyräs, J. Haddock, M. Giridhar, G. Williby, J. Schwiegerling, G. Meredith, B. Kippelen, S. Honkanen, and N. Peyghambarian, *Proc. Natl. Acad. Sci. U.S.A.* **103**, 6100 (2006).
14. X. Deng, X. Liang, Z. Chen, W. Yu, and R. Ma, *Appl. Opt.* **25**, 377 (1986).